Published in final edited form as:
Diabetes. 2005 April ; 54(4): 1064–1073.

Neuronatin, a Downstream Target of BETA2/NeuroD1 in the Pancreas, Is Involved in Glucose-Mediated Insulin Secretion

Khoi Chu[1] and **Ming-Jer Tsai**[1,2]

1 *From the Department of Molecular and Cellular Biology, Baylor College of Medicine, Houston, Texas, and the*

2 *Developmental Biology Program, Baylor College of Medicine, Houston, Texas.*

Abstract

BETA2 (NeuroD1) is a member of the basic helix-loop-helix transcription factor family. BETA2 plays an important role in the development of the pancreas and the nervous system. Using microarray technology, we identified neuronatin (*Nnat*) as differentially expressed between wild-type (WT) and knockout (KO) pancreatic RNA from embryonic day 14 (e14.5). NNAT is a member of the proteolipid family of amphipathic polypeptides and is believed to be involved in ion channel transport or channel modulation. Northern blot and in situ hybridization analysis of WT and KO samples confirmed the downregulation of *Nnat* in pancreas of mutant *BETA2* embryos. Chromatin immunoprecipitation and gel shift assays were performed and demonstrated the presence of BETA2 on the *Nnat* promoter, thus confirming the direct transcriptional regulation of *Nnat* by BETA2. To assess NNAT potential function, we performed knockdown studies by siRNA in NIT cells and observed a reduction in the ability of the NIT cells to respond to glucose. These results suggest for the first time an important role for NNAT in insulin secretion and for proper β-cell function.

Keywords

CHIP, chromatin immunoprecipitation assay; NNAT, neuronatin; RIA, radioimmunoassay; SSC, sodium chloride–sodium citrate; TBS-X, Tris-buffered saline with 0.1%Triton

BETA2/NeuroD1 (hereinafter referred to as BETA2), a member of the basic helix-loop-helix transcription factor family, was cloned as a regulatory factor for the transcription of the insulin gene and also as a neuronal differentiation factor (1,2). In addition to its function in pancreas development, BETA2 plays a role in neuronal development in the hippocampus, inner ear, cerebellum, retina, and pituitary (3–8). BETA2 is important for the proper development and differentiation of pancreatic endocrine cells (9). Targeted disruption of the mouse *BETA2* gene leads to neonatal lethality due to severe diabetes and ketoacidosis (6,9). The postnatal lethality is observed in C57BL/6, mixed C57BL/6–129SvJ, and ICR mouse strains. However, in the 129SvJ strain, ~40% of knockout (KO) pups do not exhibit keto-acidosis and survive into adulthood (5,10). In the mouse, *BETA2* is detected first at embryonic day 9.5 (e9.5) in few cells of the forming pancreatic bud (9). Thereafter, *BETA2* expression increases as endocrine cells are generated and becomes restricted to islet cells in adult mice (9). A detailed embryonic analysis of *BETA2* KO embryos has revealed a normal proliferation of *BETA2* positive/ endocrine cells during early and mid-gestation (e9.5–e16.5), but a dramatic elevation of apoptosis and an associated cease of expansion of endocrine cells at e17.5 (9). In addition, the surviving KO mice had mild hyperglycemia and an impaired glucose tolerance test (10). Taken

Address correspondence and reprint requests to Ming-Jer Tsai, PhD, Department of Molecular and Cellular Biology, Baylor College of Medicine, One Baylor Plaza, Houston, TX 77030. E-mail: mtsai@bcm.tmc.edu.

together, these results suggest a role for BETA2 in the maintenance and/or maturation of pancreatic endocrine cells.

Neuronatin (NNAT) is a member of the proteolipid protein family and is believed to be a membrane protein (11–13). *Nnat* is also an imprinted gene that is expressed from the paternal allele (14,15). *Nnat* maps to 20q11.2–q12 in humans and chromosome 2 (band 2H1) in mice. *Nnat* is highly expressed in postmitotic neurons (11,13,16), especially in the neonatal brain, with a subsequent decrease in expression levels in the adult brain (11,16). Two major splicing variants of NNAT encoding for 81 (α isoform) and 54 (β isoform) amino acids (11,12) have been described. In the adult mouse, *Nnat* is expressed in the brain, pituitary gland, lungs, adrenal glands, uterus, skeletal muscles, ovaries, and pancreas (13,17–19). It is interesting that *Nnat* is highly expressed in the β-cell lines βTC1 and βTC3 (17,18). Although many studies have been published on *Nnat*, no physiological function has yet been described for *Nnat*.

In the present study, we identified *Nnat* as a target gene of BETA2 in the pancreas. In situ hybridization, Northern blot, and immunohistochemical analyses indicate that *Nnat* is expressed in the developing and adult islet of the pancreas. Chromatin immunoprecipitation (CHIP) and gel shift assays demonstrated the presence of BETA2 binding sites at the *Nnat* promoter. Finally, siRNA knockdown of *Nnat* expression in NIT cells led to a decrease in glucose-mediated insulin secretion. This is the first report for a physiological function for NNAT in β-cells.

RESEARCH DESIGN AND METHODS

RNA isolation.

The pancreas from e14.5 embryos was isolated in RNAlater (Ambion) and kept in Trizol at −80°C. Generation of the BETA2 null mutant and PCR primers for genotyping have been previously published (9). Each embryo was genotyped by PCR, and KO-positive DNA was further confirmed by Southern blot analysis. In all, 10–12 pancreases of the same genotype were pooled and total RNA was extracted using Trizol reagent (Invitrogen, Carls-bad, CA) and purified on an RNeasy spin column (Qiagen, Valencia, CA). Total RNA from β-TC3, α-TC1, NIT, and ARIP cells was purified with Trizol. A total of six Affymetrix MG_U74Av2 chips were probed (three wild-type [WT] and three KO chips) with cRNA generated from 10 μg of total RNA. Hybridization and scanning of the chips were performed by the Molecular Genomics Core at the University of Texas Medical Branch (Galveston, TX). Software used for the analysis included DChip (www.dchip.org) and S+ArrayAnalyzer (Insightful).

Total RNA for Northern blot analysis.

Total RNA of each genotype was loaded on a denaturing agarose gel containing 0.8 mol/l formaldehyde and transferred to a BioDyne B nitrocellulose membrane. The efficiency of the transfer was assessed by methylene blue staining. This staining is reversible through incubation with the hybridization buffer and does not appear to interfere with the hybridization process. Probes were generated using a NEBlot random labeling kit (New England Biolabs), and hybridization was performed with UltraHyb solution (Ambion) at 50°C. Membranes were washed twice with 2 × sodium chloride–sodium citrate (SSC), 0.1% SDS at 50°C, and twice with 0.1 × SSC, 0.1% SDS (50°C), and then exposed to BioMax film. Densitometry quantification was performed using ImageJ software (National Institutes of Health).

Immunohistochemistry, immunocytochemistry, and in situ hybridization.

Embryos were fixed overnight in formalin at 4°C and embedded in paraffin. Adult pancreases were fixed in Bouin fixation buffer. Sections were cut at 7 μm. In situ hybridization was performed as previously described using ^{35}S– or ^{33}P-UTP–labeled probes (20). For the

immunocytochemistry studies, NIT cells were grown on microscope slides and fixed with methanol (−20°C) for 10 min at room temperature. After PBS washes, cells were permeabilized with 0.2% Triton-PBS (PBS-X) for 10 min.

Immunohistochemistry was performed as follows. Slides were dewaxed and washed in PBS (three times at 5 min). Microwave antigen retrieval was performed in Antigen Retrieval Citra solution (Biogenex). The slides were permeabilized with PBS-X for 10 min and blocked in 10% normal donkey or goat serum and 1% BSA for 30 min. Controls used to determine signal specificity included either omitting the primary antibody or using the appropriate species IgG. Primary antibodies were incubated overnight at 4°C in PBS containing 1% serum and 0.1% BSA. The dilution and detection of the primary antibodies are summarized in Table 1. Slides were washed in Tris-buffered saline with 0.1% Triton (TBS-X; Sigma) containing TBS-X (three times at 5 min) and incubated with the appropriate secondary antibodies for 30 min at room temperature. Slides were washed in TBS-X (three times at 5 min) and mounted with Slow-Fade with DAPI (Molecular Probes). Tyramide signal amplification was performed as described by the manufacturer (Molecular Probes). Slides were examined under epifluorescence using a Axioskop 2 microscope. Confocal microscopy images were captured with a Zeiss LSM 510 META Confocal Microscope. Images were captured using the AxioVision imaging software and further processed using Photoshop 7.01 (Adobe).

Knockdown of *Nnat* by siRNA and radioimmunoassay for insulin.

The siRNA for *Nnat* were designed by Dharmacon using their Smart Pool service. The Smart Pool siNNAT was introduced into NIT cells using the double electroporation protocol. On day 1, cells were electroporated and allowed to rest for 3 days; on the 3rd day, cells were re-electroporated and again allowed to rest for 3 days, after which a radioimmunoassay (RIA) was performed. Briefly, 10 million cells were resuspended in 1 ml of PBS. Smart Pool siNNAT was added to the cells at a final concentration of 100 nmol/l. One pulse of 0.4 mV (250 μF) was applied. Cells were then plated onto a 10-cm dish containing Dulbecco's modified Eagle's medium (10% FCS). The same electroporation protocol was repeated 3 days later. Cells were then plated at 500,000 cells per well in a 12-well plate in triplicate for further studies by RIA. Another 1 million cells were plated onto a well of a 6-well plate, and RNA was extracted from these cells for confirmation of siRNA knockdown by Northern blot.

The RIA for insulin was performed as described by Wang et al. (21). The RIA kit was obtained from Linco Research.

Chromatin immunoprecipitation assays.

CHIP assays were performed as described in Yoon et al. (22). The CHIP assays were then performed with two antibodies against BETA2 (G20 and N19 from Santa Cruz Biotechnology). For PCR, 1 μl from a 50-μl DNA extraction and 30–35 cycles of amplification were used. The primers used for PCR were as follows: MS Insulin I-S-296, TCAGCCAAAGATGAAGAAGGTCTC; MS Insulin I-AS-126, TCCAAACAGTT GCCTGGTGC; NNAT-S-1, AGCGGACTCCGAGACCAGTA; NNAT-AS+205, AT GGATTAAGGGGTCCCGGG; NNAT-S-644, AAGCTCGCTCCTTTGGCACA; NNAT-AS-360, GGATGGAAAGCCGAAGTTACA; NNAT-S-1,201, TTGCCTTTTGCAAATAGTTCAGC; NNAT-AS-1040, CTTTCATAGACCCATTTCTGTTCAA; NNAT-S-2245, TCTCGGCAGACGTTAGGTGC; NNAT-AS-2082, GGAACGGAAACCTTGCACAA; NNAT-S-3005, ATACTGCACATCTCCCTCCTG; NNAT-AS-2750, TCCTTCGTTCCCTTTTGAGA; PCK-S-434, GAGTGACACCTCACAGC TGTGG; and PCK-AS-96, GGCAGGCCTTTGGATCATAGCC.

Gel shift assay.

BETA2 and E47 were cotranslated in vitro using the TNT Quick Coupled Transcription/Translation Systems (Promega). We incubated 1 μl of the translation product with ~50,000 cpm of Klenow-labeled, double-stranded oligonucleotides, corresponding to the putative E-boxes, in 15 μl of binding buffer (20 mmol/l Tris-HCl [pH 7.5], 5 mmol/l $MgCl_2$, 100 mmol/l KCl, 10% glycerol, 0.01% Triton X100, and 0.5 μg polydI-dC). Incubation was performed on ice and, when indicated, 2 μl (400 ng) of goat α-BETA2 (N19; Santa-Cruz) was included in the binding buffer. The binding reaction was loaded onto a 4% polyacrylamide gel with 0.5% glycerol in 0.5 × Tris borate EDTA buffer. The oligonucleotide sequences were as follows: GATCCTTC CGCGTGCTGCTGCAGGTGAGTATGTACCCGGGCTTT, +1/−205-S; GATCA AAGCCCGGGTACATACTCACCTGCAGCAGCACGCGGAAGGATC, +1/−205-AS; GATCCAAGATTCTCACAAAACAGCTGGCATGGGTTTAAAA, −644/−360-S; GATCTTTTAAACCCATGCCAGCTGTTTTGTGAGAATCTTG, −644/−360-AS; GATCCCACAATACCCAAACTCAGTTGGACCATTAAACC, −1,201/−1040-S; GA TCGGTTTAATGGTCCAACTGAGTTTGGGTATTGTGG, −1,201/−1040-AS; and GATCCGGATCAGCAGATGGCCAGAGGGGCTA, RIPE3a-AS.

RESULTS

Profiling of transcription factors in the developing pancreas of BETA2 mutant embryos.

To further define the effects of the lack of BETA2 in the developing pancreas, we performed a detailed immunostaining study for important pancreatic transcription factors. We have previously shown that in the absence of BETA2, a decrease in endocrine cells is observed around e15.5 and culminates with an ~50–60% decrease in endocrine cells at e17.5-P0 due to extensive apoptosis. Thus, e14.5 pancreases from WT and KO embryos were stained with BETA2, β-galactosidase, Pdx1, Ngn3, Pax6, Nkx6.1, and Nkx2.2. At this stage, BETA2 was detected in few cells adjacent to epithelial duct cells in the WT but not the KO pancreas (Fig. 1*A* and *B*) and, conversely, β-galactosidase, which replaces the BETA2 gene locus in the KO, was detected only in the KO and not the WT pancreas (Fig. 1*C* and *D*). We did not observe any major differences in staining between the WT and KO embryos in all the other transcription factors studied (Fig. 1*E–N*). In addition, a counting of Ngn3-positive (an upstream gene of BETA2) and Pax6-positive (a potential downstream gene of BETA2) cells did not reveal any statistical differences (data no shown). Furthermore, immunostaining for two cell adhesion molecules (Ep-CAM and E-CAD) did not reveal any difference between the WT and KO embryos at e14.5 (data not shown). These results suggest that e14.5 is an ideal age at which to identify potential target genes of BETA2 without the negative aspect of apoptosis.

Neuronatin expression is dramatically decreased in BETA2 mutant pancreas.

DNA microarray analysis was performed to identify potential BETA2 target genes by comparing RNA samples from e14.5 *BETA2* WT with those from KO pancreases. Consistent with the function of *BETA2* in endocrine differentiation, BETA2, insulin, and glucagon transcripts were found to be downregulated, which seems to validate this approach for *BETA2* target gene discovery. Among the genes identified, *Nnat* was dramatically reduced in the KO samples and was chosen for further studies, in light of its expression in neurons and β-cell lines.

The validity of *Nnat* as a target of *BETA2* was assessed by in situ hybridization and Northern blot analysis. From in situ hybridization, *Nnat* transcripts were detected in WT pancreases from both e14.5 and e16.5, whereas no transcripts were observed in KO pancreases (Fig. 2*A–D* and *I–L*). In KO embryos, the absence of *Nnat* transcripts in the pancreas appears to be specific to this tissue, as *Nnat* was detected in the developing pituitary gland and cerebellum at levels comparable with those observed in WT embryos (Fig. 2*E–H* and data not shown). To confirm

that the absence of *Nnat* transcript is not due to the absence of endocrine cells on the section analyzed, the adjacent section was hybridized with a probe encoding for *GLUT2*, a marker for endocrine cells in the pancreas. *GLUT2* transcript was detected on both the WT and the KO pancreases (Fig. 2*M–P*), with no apparent difference in expression. In addition, *Nnat* transcripts were clearly absent from KO RNA samples at e16.5, as measured by Northern blot analysis (Fig. 3*A*). This decrease was paralleled by a marked reduction in insulin and glucagon transcripts, two known target genes of *BETA2* (Fig. 3*B*), whereas the expression of the exocrine marker amylase was unaltered (Fig. 3*C*). Furthermore, transcripts for *Nnat* were also reduced in the eye of postnatal day 1 pups. These results indicated that *Nnat* is downregulated in two tissues where BETA2 has important developmental function.

Chromatin immunoprecipitation assay of the NNAT promoter and gel shift assays.

A CHIP assay was performed to determine if *Nnat* is a direct target of BETA2. The cell line βTC3 was used because it expresses high levels of *Nnat* mRNA (Fig. 4*A*). The CHIP assay was performed with two antibodies against BETA2 (G20 and N19), with a similar outcome. Specific PCR amplification was obtained after precipitation with anti-BETA2 antibodies, but not when goat IgG was used. All regions selected for PCR contained potential E-box (CANNTG) binding sites. Only the proximal *Nnat* promoter was efficiently precipitated and amplified (Fig. 4*B*, *lanes NNAT[−1, +205]*, *NNAT[−664, −360]*, and *NNAT[−1,201, −1,040]*), whereas the distal *Nnat* promoter was not amplified (Fig. 4*B*, *lanes NNAT[−2,245, −2082]* and *NNAT[−3,005, −2,750]*). As a positive control, the insulin promoter, which contains BETA2 binding sites, was precipitated and amplified, whereas a nonregulated promoter, the *PEPCK* gene, was not. To further confirm the CHIP results, we performed gel shift assay using the in vitro–translated BETA2/E47 protein complex and the E-boxes from the three positive regions identified by the CHIP assay. Strong binding to the E-box located in the NNAT(−664, −360) region was seen, whereas weak or no binding was observed for the E-boxes present in the NNAT(−1, +205) and NNAT(−1,201, −1,040) regions (Fig. 4*C*). In addition, gel shift experiments with the E-boxes that were not positive in the CHIP assay were also negative for binding to BETA2 in the gel shift assay (data not shown). The presence of BETA2 in the retarded complex was confirmed by antibody supershift (Fig. 4*C*, "+" *lanes*), whereas control goat IgG did not (Fig. 4*C*, "–" *lanes*). It was interesting to note that the intensity of the binding for the *NNAT* (−664, −360) E-box was similar to that of the classical E-box present on the RIPE3a enhancer of the insulin promoter.

Developmental expression of neuronatin in the pancreas.

We next performed a detailed developmental analysis of *Nnat* expression in the pancreas by in situ hybridization and Northern blot. At e12.5, *Nnat* was detected in a few pancreatic cells (Fig. 5*A*), whereas the number of *Nnat*-expressing cells increased dramatically by e14.5 (Fig. 5*B*). Of interest, *Nnat*-expressing cells were found adjacent to ductal epithelial cells (Fig. 5*B*, red arrow) or in cell aggregates (Fig. 5*B*, black arrow), suggesting that *Nnat* is expressed in differentiating endocrine cells and early aggregating islet cells. *Nnat* expression gradually increases by e16.5 (Fig. 5*C*), paralleling the development of endocrine cells. By e18.5 (Fig. 5*D*), *Nnat* expression was restricted to the central core of the forming islet (data not shown). Immunohistochemical localization demonstrated the presence of NNAT in the central core of an islet of Langerhans in the adult pancreas; such a pattern indicates that it is located in β-cells similar to BETA2. Northern blot analysis using embryonic pancreatic and postnatal RNA samples was performed and confirmed the steady increase of *Nnat* during pancreas development (Fig. 5*F*). Thus, the expression profile of *Nnat* parallels BETA2's profile and suggests a potential role for *Nnat* in the development of endocrine cells.

NNAT localization in the NIT β-cell line.

To gain further insight into the function of NNAT, we performed immunocytochemistry to localize the NNAT protein in the insulinoma cell line NIT, which expresses high levels of *Nnat* RNA (Fig. 4*A*). Using confocal microscopy, NNAT was localized to the cytoplasm (Fig. 6*B*). Insulin was also consistently colocalized to the cytoplasm (Fig. 6*A*). The merging of the two images suggests a potential colocalization of NNAT and insulin, but further experiments are required to definitely confirm the colocalization. Furthermore, attempts to detect NNAT proteins in the medium were unsuccessful, indicating that NNAT is unlikely to be a secreted protein (data not shown).

Role of NNAT in insulin secretion.

We next tested the potential role for NNAT in β-cell's main function, that is, insulin secretion in response to glucose. To test our hypothesis, we performed siRNA experiments to knockdown *Nnat* in NIT cells. The introduction of siRNA against *Nnat* (siNNAT) into NIT cells led to the knockdown of *Nnat* mRNA when compared with controls (siGFP) (Fig. 7*A*). As a control for the specificity for the knockdown, Northern blot for insulin transcripts did not change between control (siGFP) and siNNAT (Fig. 7*A*).

Electroporation had no effect on NIT's ability to secrete insulin, as unelectroporated cells responded to similar levels as the electroporated cells (Fig. 7*B*, compare electroporation control vs. untreated cells). When NIT cells were challenged with glucose, a 7- to 15-fold increase in secreted insulin was observed (Fig. 7*B*, siGFP, electroporation control, and untreated cells), whereas only a 2.7-fold increase was observed when *Nnat* was knocked down (Fig. 7*B*, siNNAT). Hence, it seems that the inhibition is specific to the downregulation of NNAT, rather than to nonspecific effects impacting on granule transport or exocytic events. Taken together, these results suggest an important function for NNAT in insulin secretion.

DISCUSSION

BETA2 is an important factor for pancreatic endocrine cell terminal differentiation and survival (9). BETA2 is believed to regulate genes important for mature β-cell function. It is not surprising that BETA2 is an important regulator of insulin and glucagon gene transcription (1,23). Furthermore, surviving KO mice have an impaired glucose tolerance test, suggesting a defect in either glucose sensing or insulin secretion (10). The importance of BETA2 is highlighted by the discovery that it is the sixth maturity-onset diabetes of the young (*MODY6*) gene identified (24). In addition, many genetic studies in various populations have linked mutations in BETA2 to susceptibility to type 1 (25–27) and type 2 (28,29) diabetes. Consequently, target genes of BETA2 will likely affect the etiology of diabetes linked to *BETA2*. To identify potential target genes of BETA2 in the pancreas, we performed a microarray screening of embryonic pancreatic RNA. Based on our previously described results, endocrine cell development is perturbed during late gestation (9); thus, we used e14.5 as a working time point for the microarray studies. We found 216 genes that varied by at least 1.5-fold, with 66 genes downregulated and 150 genes upregulated in the KO samples. We also found many metabolic hormones (insulin, glucagon, gastrin, and neuropeptide Y) downregulated in the KO pancreases. We observed that 11 transcription factors were higher in the WT samples, including BETA2, *Nfatc1*, Kruppel-like factor 7, *Pbx1*, and *Paraxis*. Of interest, Pbx1 was recently shown to be required for pancreas development (30). Numerous genes involved in cytoskeleton/intracellular/intracellular matrix formation were also downregulated in the mutant pancreases (e.g., *lamin-B1*, *actinin-α1*, *matrilin 4*); this observation is consistent with the high state of proliferation and migration that occurs at this age. Finally, many molecules involved in signaling were identified, including *Notch1*, *IRS 2*, *Rap1*, and *Nnat*. We were surprised to identify more genes upregulated in the KO samples

acting on diverse biological pathways. Of interest, numerous genes involved in apoptosis were upregulated in the KO samples, such as *Bnip2*, *Bnip3l*, and *Pdcd6*/*Alg2*. The upregulation of pro-apoptosis genes is consistent with the KO phenotype.

The identification of *Nnat* as a target gene of BETA2 fits well with this premise, as it appears to play a role in insulin secretion. NNAT shows weak homology to phospholamban and PMP1, two proteolipid family members that function as a Ca^{2+}-ATPase and H^{+} ATPase, respectively (31,32).

In the pancreas, *Nnat* is present as early as e12.5 in a few cells and increases gradually; from e14.5 to e18.5, there is a dramatic expression in endocrine cells (Fig. 5*A–D*). This increase is reminiscent of the appearance of BETA2 and insulin in the pancreas (9). Furthermore, NNAT was detected by immunohistochemical methods in islets of the adult pancreas (Fig. 5*F*). NNAT was detected in the central core of the islet, which is indicative of its presence in mostly β-cells; however, its presence in the other endocrine cell types cannot be excluded. In addition, *Nnat* mRNA expression persists in the postnatal and adult pancreas (Fig. 5*G*).

The expression of *Nnat* was assessed in *BETA2* WT and KO pancreas from e14.5 and e16.5 by in situ hybridization and Northern blot analysis. By in situ hybridization, *Nnat* was readily detected in the pancreas of WT embryos at e14.5 and e16.5, whereas it was undetectable in KO embryos (Fig. 2*A–D* and *I–L*). Similar results were obtained by Northern blot analysis (Fig. 3*A*). Furthermore, *GLUT2* was detected in both WT and KO e16.5 embryos, thereby confirming the presence of endocrine cells in the KO sections (Fig. 2*M–P*). The decrease of *Nnat* observed by Northern blot analysis also parallels the decrease in insulin and glucagon transcripts, two known targets of BETA2, in the KO samples, whereas the level of amylase, a marker for exocrine cells, was unchanged in the KO pancreas (Fig. 3*C*). In addition, *Nnat* transcripts were also reduced in the developing eye (Fig. 3*D*), whereas no difference was observed in the developing cerebellum (data not shown). Although the function of NNAT in the retina is unknown, its temporal and expression patterns in the retina (33) suggest that *Nnat* is expressed in amacrine cells, where BETA2 is known to play a role in cell fate specification (34,35). The observation of the downregulation of *Nnat* in two BETA2-expressing tissues indicates the relevance of this target gene. Finally, the immunohistochemistry of numerous transcription factors important for endocrine cells genesis and/or differentiation does not suggest a general downregulation of endocrine cells at e14.5 (Fig. 1), but does indicate that the downregulation of *Nnat* is specific.

CHIP assay suggests that indeed *Nnat* is a direct target of BETA2 (Fig. 4*B*). BETA2 was able to bind to multiple regions proximal to the transcriptional start site, but failed to precipitate the more downstream chromatin regions NNAT(−2,245, −2082) and NNAT(−3,005, −2750). All the E-boxes located in the targeted regions contained the core consensus E-box CANNTG (Fig. 4*D*). Thus, other determinants, such as the sequence of the two variable nucleotides in the central core of the E box consensus and flanking sequences of the E-box, will likely confer specificity and affinity. Gel shift experiments were performed with the E-boxes from the three regions that were positive on the CHIP assay. Strong binding to the E-box located in the NNAT (−664, −360) region was observed, comparable with the classic RIPE3a binding site in the insulin promoter. Only weak or no binding was observed for the E-boxes present in the NNAT (−1, +205) and NNAT(−1,201, −1040) regions, respectively. The weak or lack of binding of these two E-boxes identified by the CHIP assay could be due to *1*) the E-boxes and their flanking sequences, *2*) the requirement for a specific interacting partner/environment present only in vivo, or *3*) the limitation of the CHIP assay in defining the exact E-box when they are in close proximity (i.e., 400–800 bp), which is directly linked to the chromatin size generated by the sonication step. One interesting observation was the correlation between the CHIP and

gel shift assay results, in that a strong binding in gel shift corresponded to an efficient CHIP assay (Fig. 4*B* and *C*, *lanes NNAT[−644, −360]* and *insulin/RIPE3a*).

Immunocytochemistry for NNAT was performed on NIT cells. NIT cells express high levels of *Nnat* mRNA (Fig. 4*A*). By confocal microscopy, insulin and NNAT were localized in the cytoplasm (Fig. 6*A* and *B*). Although the merge figure (Fig. 6*C*) suggests the possible colocalization of NNAT with insulin, the definite colocalization will require a more detailed analysis using electron microscopy. We tested if NNAT was important for secretion; to do so, we knocked down *Nnat* using siRNA. Knockdown of *Nnat* in NIT cell did not have a significant effect on basal insulin secretion, but did lead to impaired response in the presence of glucose (Fig. 4*B*). The result indicates a potential role for NNAT in insulin secretion in response to glucose. This is the first report of a physiological function for NNAT.

BETA2 is a transcription factor important for neuronal and endocrine cell terminal differentiation and/or survival. Thus, it is quite appropriate that *Nnat* is a target gene for BETA2, given that *Nnat* is expressed in both neurons and β-cells of the pancreas. NNAT does indeed appear to play a role in mature β-cells, whose main function is insulin secretion in response to glucose. The latter finding is consistent with the impaired glucose tolerance test observed in the surviving KO mice (10). It is interesting that in naturally occurring mice that lack *Nnat* (MatDp. dist2. T26H), there is a decrease in insulin staining with an accumulation of insulin signal adjacent to the nucleus in newborn pancreas when compared with controls (K.C., M.-J.T., C.V. Beechey, J. Peters, unpublished observations); this finding is suggestive of incorrect sorting or impaired trafficking of secretory vesicle. Furthermore, in a rat model with impaired glucose mediated insulin secretion, *Nnat* has been identified as downregulated in islets (36). The authors of the latter study overlooked the importance of such a finding, as no function was assigned to *Nnat*.

In conclusion, the present data show that *Nnat* is a direct target gene of BETA2 and, more importantly, its role in glucose-mediated insulin secretion. The potential role for NNAT in diabetes should be an attractive avenue for further studies.

Acknowledgements

M.-J.T. is supported by National Institutes of Health Grant HD-17379.

We thank Eric Némoz-Gaillard, Debra Bramblett, Luoping Li, and Sophia Tsai for a critical reading of the manuscript and helpful discussions.

References

1. Naya FJ, Stellrecht CM, Tsai MJ. Tissue-specific regulation of the insulin gene by a novel basic helix-loop-helix transcription factor. Genes Dev 1995;9:1009–1019. [PubMed: 7774807]
2. Lee JE, Hollenberg SM, Snider L, Turner DL, Lipnick N, Weintraub H. Conversion of Xenopus ectoderm into neurons by NeuroD, a basic helix-loop-helix protein. Science 1995;268:836–844. [PubMed: 7754368]
3. Liu M, Pereira FA, Price SD, Chu MJ, Shope C, Himes D, Eatock RA, Brownell WE, Lysakowski A, Tsai MJ. Essential role of BETA2/NeuroD1 in development of the vestibular and auditory systems. Genes Dev 2000;14:2839–2854. [PubMed: 11090132]
4. Kim WY, Fritzsch B, Serls A, Bakel LA, Huang EJ, Reichardt LF, Barth DS, Lee JE. NeuroD-null mice are deaf due to a severe loss of the inner ear sensory neurons during development. Development 2001;128:417–426. [PubMed: 11152640]
5. Liu M, Pleasure SJ, Collins AE, Noebels JL, Naya FJ, Tsai MJ, Lowenstein DH. Loss of BETA2/NeuroD leads to malformation of the dentate gyrus and epilepsy. Proc Natl Acad Sci U S A 2000;97:865–870. [PubMed: 10639171]

6. Miyata T, Maeda T, Lee JE. NeuroD is required for differentiation of the granule cells in the cerebellum and hippocampus. Genes Dev 1999;13:1647–1652. [PubMed: 10398678]
7. Pennesi ME, Cho JH, Yang Z, Wu SH, Zhang J, Wu SM, Tsai MJ. BETA2/NeuroD1 null mice: a new model for transcription factor-dependent photoreceptor degeneration. J Neurosci 2003;23:453–461. [PubMed: 12533605]
8. Lamolet B, Poulin G, Chu K, Guillemot F, Tsai MJ, Drouin J. Tpit-independent function of NeuroD1 (BETA2) in pituitary corticotroph differentiation. Mol Endocrinol 2004;18:995–1003. [PubMed: 14726486]
9. Naya FJ, Huang HP, Qiu Y, Mutoh H, DeMayo FJ, Leiter AB, Tsai MJ. Diabetes, defective pancreatic morphogenesis, and abnormal enteroendocrine differentiation in BETA2/NeuroD-deficient mice. Genes Dev 1997;11:2323–2334. [PubMed: 9308961]
10. Huang HP, Chu K, Nemoz-Gaillard E, Elberg D, Tsai MJ. Neogenesis of beta-cells in adult BETA2/NeuroD-deficient mice. Mol Endocrinol 2002;16:541–551. [PubMed: 11875114]
11. Joseph R, Dou D, Tsang W. Molecular cloning of a novel mRNA (neuronatin) that is highly expressed in neonatal mammalian brain. Biochem Biophys Res Commun 1994;201:1227–1234. [PubMed: 8024565]
12. Joseph R, Dou D, Tsang W. Neuronatin mRNA: alternatively spliced forms of a novel brain-specific mammalian developmental gene. Brain Res 1995;690:92–98. [PubMed: 7496812]
13. Wijnholds J, Chowdhury K, Wehr R, Gruss P. Segment-specific expression of the neuronatin gene during early hindbrain development. Dev Biol 1995;171:73–84. [PubMed: 7556909]
14. Kagitani F, Kuroiwa Y, Wakana S, Shiroishi T, Miyoshi N, Kobayashi S, Nishida M, Kohda T, Kaneko-Ishino T, Ishino F. Peg5/Neuronatin is an imprinted gene located on sub-distal chromosome 2 in the mouse. Nucleic Acid Res 1997;25:3428–3432. [PubMed: 9254699]
15. Kikyo N, Williamson CM, John RM, Barton SC, Beechey CV, Ball ST, Cattanach BM, Surani MA, Peters J. Genetic and functional analysis of neuronatin in mice with maternal or paternal duplication of distal Chr 2. Dev Biol 1997;190:66–77. [PubMed: 9331332]
16. Usui H, Ichikawa T, Miyazaki Y, Nagai S, Kumanishi T. Isolation of cDNA clones of the rat mRNAs expressed preferentially in the prenatal stages of brain development. Brain Res Dev Brain Res 1996;97:185–193.
17. Niwa H, Harrison LC, DeAizpurua HJ, Cram DS. Identification of pancreatic beta cell-related genes by representational difference analysis. Endocrinology 1997;138:1419–1426. [PubMed: 9075697]
18. Arava Y, Adamsky K, Ezerzer C, Ablamunits V, Walker MD. Specific gene expression in pancreatic β-cells: cloning and characterization of differentially expressed genes. Diabetes 1999;48:552–556. [PubMed: 10078555]
19. John RM, Aparicio SA, Ainscough JF, Arney KL, Khosla S, Hawker K, Hilton KJ, Barton SC, Surani MA. Imprinted expression of neuronatin from modified BAC transgenes reveals regulation by distinct and distant enhancers. Dev Biol 2001;236:387–399. [PubMed: 11476579]
20. Bramblett DE, Copeland NG, Jenkins NA, Tsai MJ. BHLHB4 is a bHLH transcriptional regulator in pancreas and brain that marks the dimesencephalic boundary. Genomics 2002;79:402–412. [PubMed: 11863370]
21. Wang H, Maechler P, Hagenfeldt KA, Wollheim CB. Dominant-negative suppression of HNF-1alpha function results in defective insulin gene transcription and impaired metabolism-secretion coupling in a pancreatic beta-cell line. EMBO J 1998;17:6701–6713. [PubMed: 9822613]
22. Yoon HG, Chan DW, Reynolds AB, Qin J, Wong J. N-CoR mediates DNA methylation-dependent repression through a methyl CpG binding protein Kaiso. Mol Cell 2003;12:723–734. [PubMed: 14527417]
23. Dumonteil E, Laser B, Constant I, Philippe J. Differential regulation of the glucagon and insulin I gene promoters by the basic helix-loop-helix transcription factors E47 and BETA2. J Biol Chem 1998;273:19945–19954. [PubMed: 9685329]
24. Kristinsson SY, Thorolfsdottir ET, Talseth B, Steingrimsson E, Thorsson AV, Helgason T, Hreidarsson AB, Arngrimsson R. MODY in Iceland is associated with mutations in HNF-1alpha and a novel mutation in NeuroD1. Diabetologia 2001;44:2098–2103. [PubMed: 11719843]
25. Iwata I, Nagafuchi S, Nakashima H, Kondo S, Koga T, Yokogawa Y, Akashi T, Shibuya T, Umeno Y, Okeda T, Shibata S, Kono S, Yasunami M, Ohkubo H, Niho Y. Association of polymorphism in

the NeuroD/BETA2 gene with type 1 diabetes in the Japanese. Diabetes 1999;48:416–419. [PubMed: 10334323]

26. Hansen L, Jensen JN, Urioste S, Petersen HV, Pociot F, Eiberg H, Kristiansen OP, Hansen T, Serup P, Nerup J, Pedersen O. NeuroD/BETA2 gene variability and diabetes: no associations to late-onset type 2 diabetes, but an A45 allele may represent a susceptibility marker for type 1 diabetes among Danes. Danish Study Group of Diabetes in Childhood, and the Danish IDDM Epidemiology and Genetics Group. Diabetes 2000;49:876–878. [PubMed: 10905500]
27. Yamada S, Motohashi Y, Yanagawa T, Maruyama T, Kasuga A, Hirose H, Matsubara K, Shimada A, Saruta T. NeuroD/BETA2 gene G→A polymorphism may affect onset pattern of type 1 diabetes in Japanese. Diabetes Care 2001;24:1438–1441. [PubMed: 11473083]
28. Malecki MT, Jhala US, Antonellis A, Fields L, Doria A, Orban T, Saad M, Warram JH, Montminy M, Krolewski AS. Mutations in NeuroD1 are associated with the development of type 2 diabetes mellitus. Nat Genet 1999;23:323–328. [PubMed: 10545951]
29. Malecki MT, Cyganek K, Klupa T, Sieradzki J. The Ala45Thr polymorphism of BETA2/NeuroD1 gene and susceptibility to type 2 diabetes mellitus in a Polish population. Acta Diabetol 2003;40:109–111. [PubMed: 12861411]
30. Kim SK, Selleri L, Lee JS, Zhang AY, Gu X, Jacobs Y, Cleary ML. Pbx1 inactivation disrupts pancreas development and in Ipf1-deficient mice promotes diabetes mellitus. Nat Genet 2002;30:430–435. [PubMed: 11912494]
31. Kawasaki-Nishi S, Nishi T, Forgac M. Proton translocation driven by ATP hydrolysis in V-ATPases. FEBS Lett 2003;545:76–85. [PubMed: 12788495]
32. MacLennan DH, Abu-Abed M, Kang C. Structure-function relationships in Ca(2+) cycling proteins. J Mol Cell Cardiol 2002;34:897–918. [PubMed: 12234762]
33. Dorrell MI, Aguilar E, Weber C, Friedlander M. Global gene expression analysis of the developing postnatal mouse retina. Invest Ophthalmol Vis Sci 2004;45:1009–1019. [PubMed: 14985324]
34. Morrow EM, Furukawa T, Lee JE, Cepko CL. NeuroD regulates multiple functions in the developing neural retina in rodent. Development 1999;126:23–36. [PubMed: 9834183]
35. Inoue T, Hojo M, Bessho Y, Tano Y, Lee JE, Kageyama R. Math3 and NeuroD regulate amacrine cell fate specification in the retina. Development 2002;129:831–842. [PubMed: 11861467]
36. Waterland RA, Garza C. Early postnatal nutrition determines adult pancreatic glucose-responsive insulin secretion and islet gene expression in rats. J Nutr 2002;132:357–364. [PubMed: 11880555]

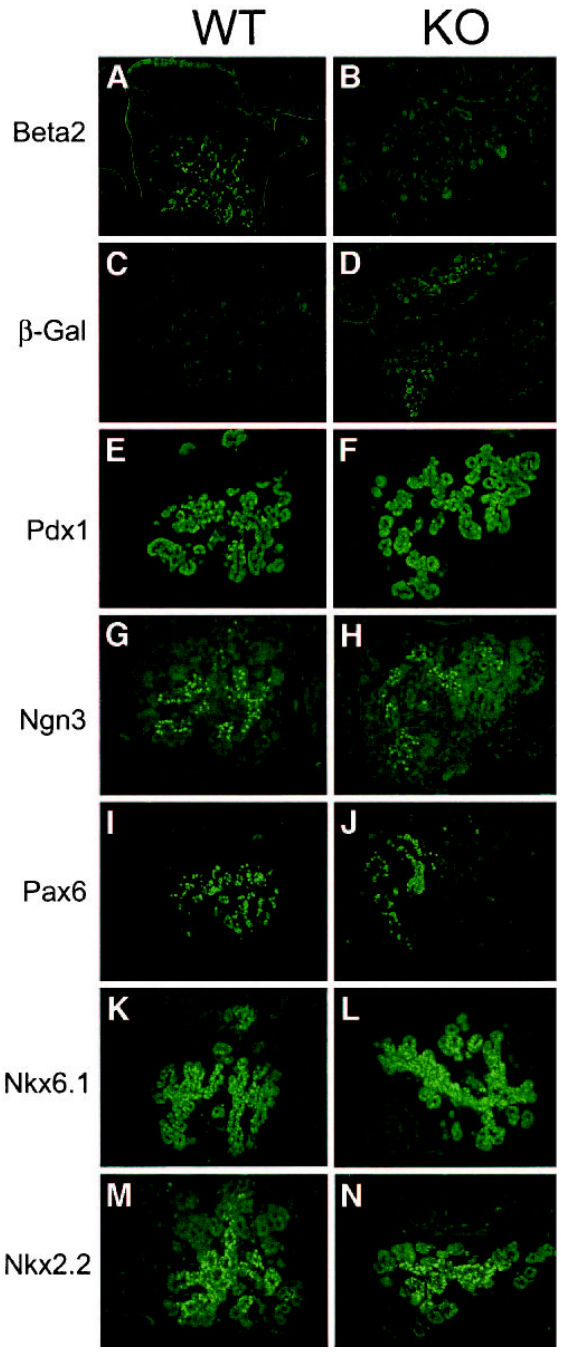

FIG 1.

Immunohistochemical profiling of important pancreatic transcription factors.

Immunohistochemistry staining of transcription factors was performed on e14.5 embryos. A representative sample of two embryos of each genotype (three slides each) is shown. BETA2 staining was observed in WT (*A*) but not in KO (*B*) samples. Conversely, β-galactosidase (β-Gal) was seen only in KO (*D*) and not in WT (*C*) pancreases. Signals for BETA2 and β-galactosidase staining were observed in a similar location adjacent to duct structure and a difference in the number was seen, indicating that BETA2 is not required for endocrine cell genesis. No difference in staining was observed for Pdx1 (*E* and *F*), Ngn3 (*G* and *H*), Pax6 (*I* and *J*), Nkx6.1 (*K* and *L*), and Nkx2.2 (*M* and *N*).

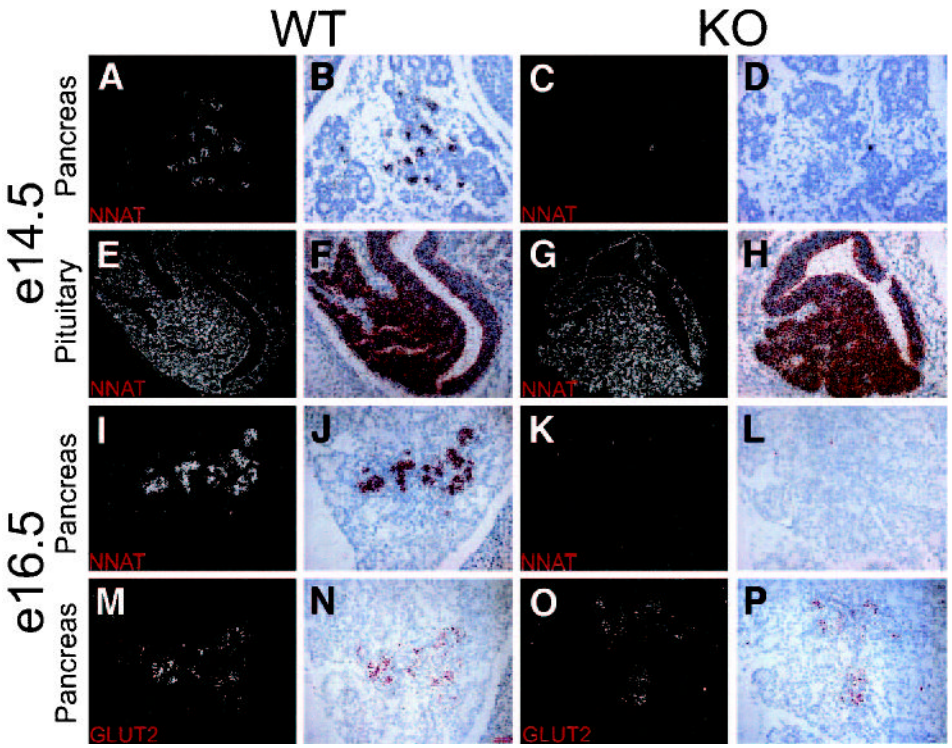

FIG 2.

In situ hybridization of *Nnat* in *BETA2* WT and KO pancreases. The in situ signals are shown in the dark field; for ease of viewing, the hematoxylin staining was overlaid with the in situ signal. The *Nnat* in situ signal was detected in e14.5 and e16.5 WT pancreas (*A*, *B*, *I*, and *J*), whereas only a weak-to-no signal was detected in KO pancreas (*C*, *D*, *K*, and *L*). A longer capture time of the *Nnat* signal on the e16.5 KO pancreases revealed a residual *Nnat* signal. In the developing pituitary, *Nnat* was detected in both WT and KO samples (*E–H*). In situ hybridization with a probe encoding for GLUT2 (*M–P*) was performed on the adjacent slide used for the *Nnat* (*I–L*) to demonstrate the presence of endocrine tissue in the pancreas at e16.5.

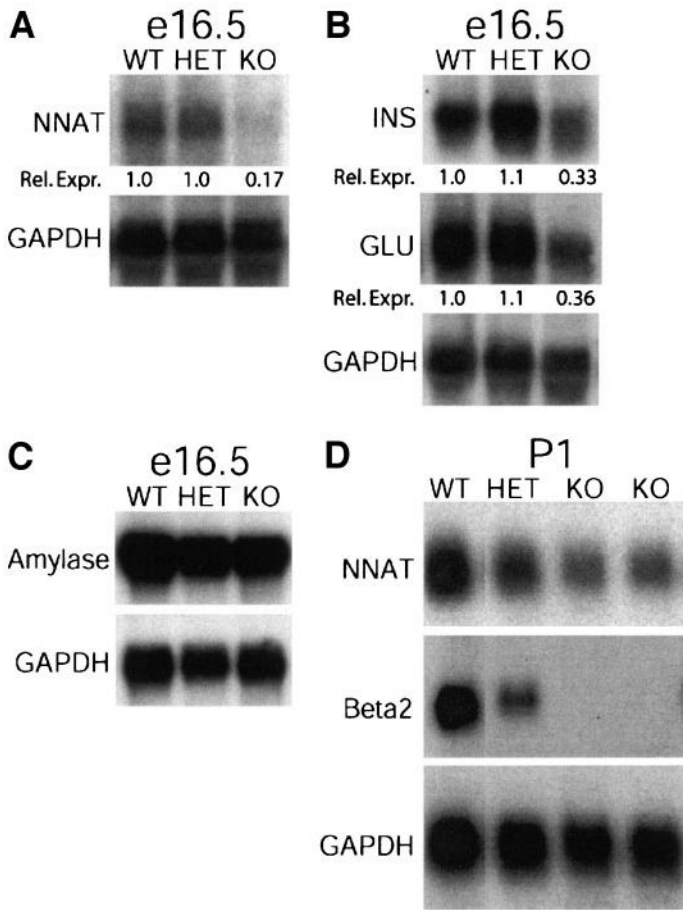

FIG 3.

Northern blot analysis of *Nnat* and pancreatic markers. Total RNA (10 μg) from e16.5 pancreas of WT and KO embryos was probed with *Nnat* (*A*), insulin (INS) and glucagon (GLU) (*B*), and amylase (*C*). *Nnat* (*A*) and INS and GLU (*B*) transcripts were readily decreased in KO samples when compared with WT or heterozygote (HET) samples. Relative expression normalized to GAPDH is shown below the blot. *D*: The Northern blot for *Nnat* using a postnatal day 1 (P1) eye shows a decrease in *Nnat* transcript in KO samples. An interesting decrease was also observed in the heterozygote sample (HET). GAPDH was used as a loading control.

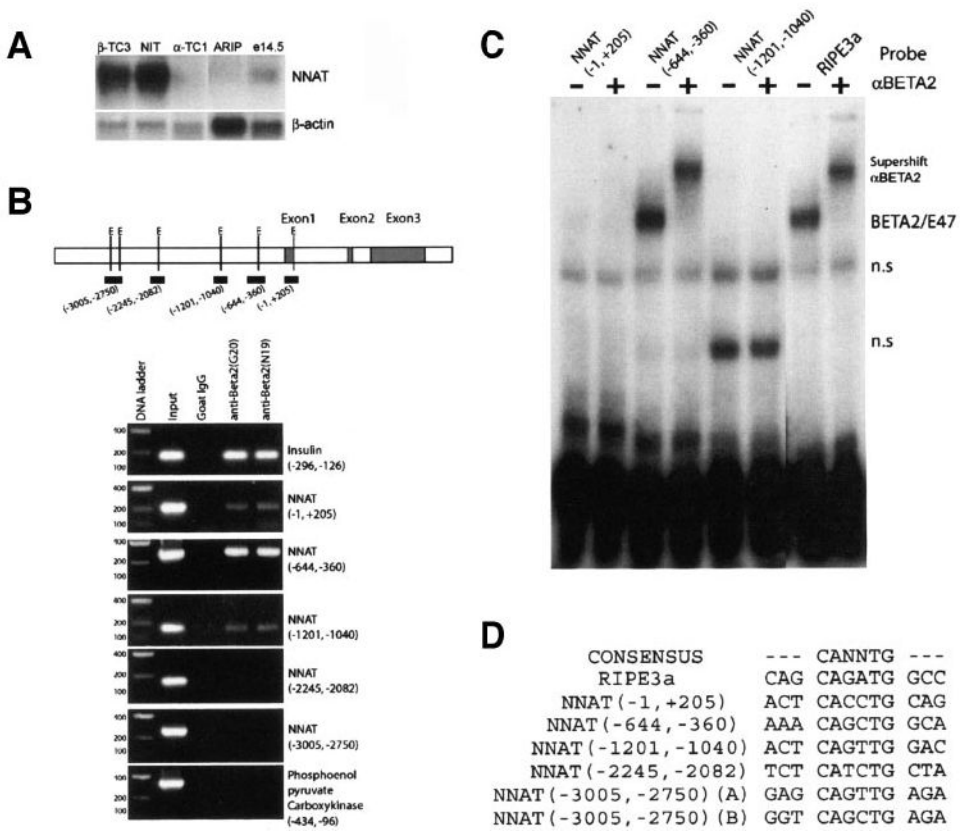

FIG 4.

Chromatin immunoprecipitation and gel shift assays. *A*: Northern blot analysis of *Nnat* mRNA in cell lines. *Nnat* is highly expressed in β-cell lines (β-TC3 and NIT), but not in the α-cell line, αTC-1, or ductal cell line, ARIP. The *Nnat* transcript level in an e14.5 embryonic pancreas is also shown. *B*: The presence of BETA2 at the *Nnat* promoter was assessed by chromatin immunoprecipitation assay (*top*). A schematic of the *Nnat* gene with its three exons is also shown (*gray box*). Potential E-boxes (E) are indicated. Genomic regions studied in the CHIP assay encompassing the putative E-boxes are shown in the black box. The DNA isolated from the CHIP protocol was amplified using specific primers. Primers to the proximal mouse insulin promoter (−296, −126) were used as a positive control for the assay. Primer pairs for the *Nnat* promoter were designed after a simple text search for the following sequence CANNTG, with one mismatch allowed. Three pairs of primers from the *Nnat* promoter efficiently amplified the correct PCR product and were located within the proximal promoter (NNAT[−1, 205], NNAT[−644, −360], and NNAT[−1201, −1040]), whereas two pairs did not amplify a PCR product (NNAT[−2,245, −2082] and NNAT[−3005, −2750]). In addition, primer pairs to a nonregulated gene (*PEPCK*) did not generate a PCR product. *C*: Electrophoresis mobility shift assay for the potential E-boxes. BETA2 and E47 proteins were cotranslated in vitro and incubated with double-stranded oligonucleotides corresponding to each of the potential E-boxes. Goat IgG (−) or goat BETA2 (+) antibodies were included to show the presence of BETA2 in the retarded complex. n.s., nonspecific binding. *D*: Alignment of the E-boxes present in the region tested in the CHIP assay.

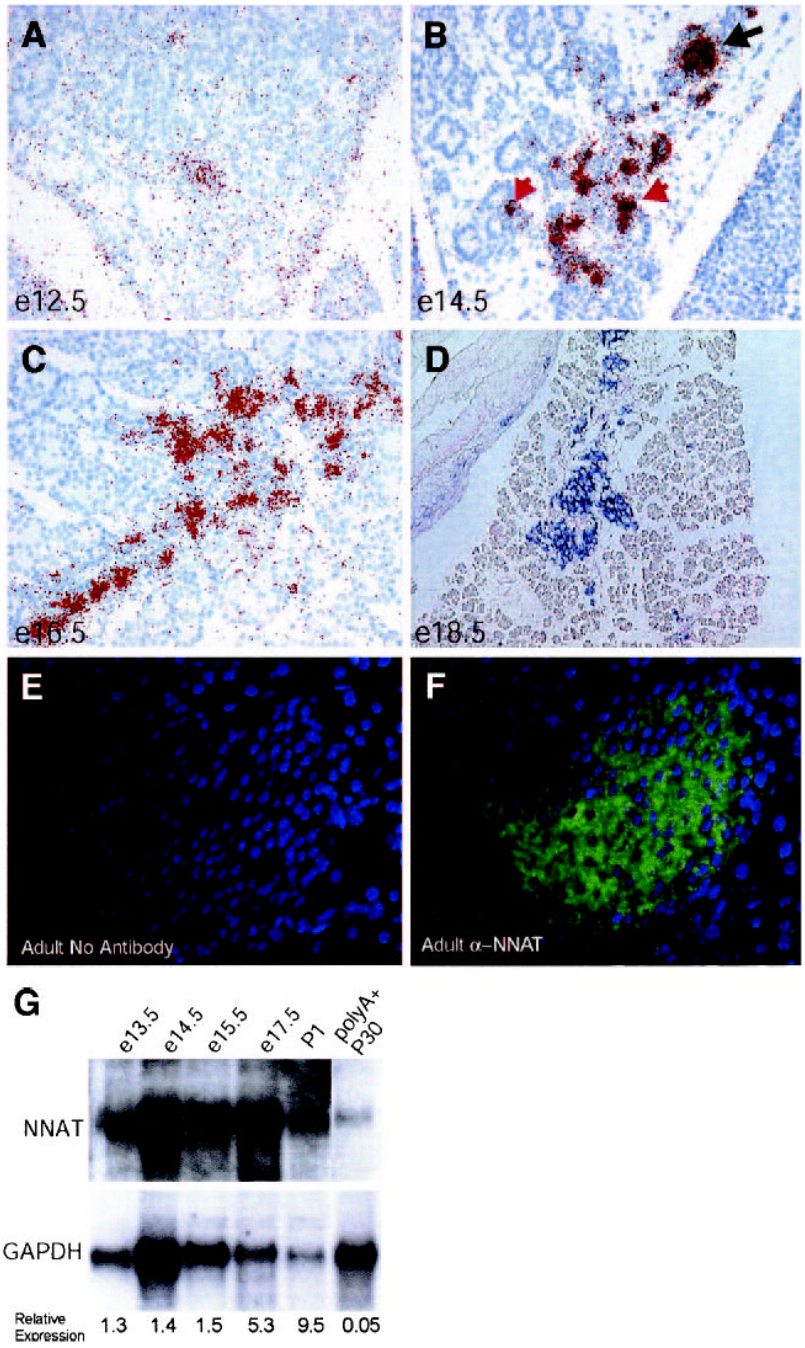

FIG 5.

Time course analysis of *Nnat* during pancreas development. In situ hybridization was performed on e12.5 (*A*,), e14.5 (*B*), e16.5 (*C*), and e18.5 (*D*) embryos. The in situ signals are artificially colored red, and for ease of viewing the hematoxylin staining was overlaid with the in situ signal (*A–C*). In *D*, the in situ hybridization was performed by nonradioactive in situ hybridization with a digoxigenin-labeled probe and detected enzymatically with NBT and BCIP. A gradual increase in *Nnat* in situ is seen from e12.5 (*A*) to e18.5 (*D*). In *B*, the *Nnat* signal can clearly be seen adjacent to epithelial duct structures (red arrow) or in endocrine clusters (black arrow). *D*: The *Nnat* in situ signal is seen in endocrine cell clusters indicative of β-cells. *E–F*: Immunohistochemical analysis of NNAT in an adult pancreas. *NNAT* is

detected in the central core of an islet, suggesting its colocalization in β-cells (*F*), whereas no signal is detected in the same islet on the adjacent section (*E*). *G*: A time course of *Nnat* mRNA by Northern blot analysis. *Nnat* mRNA was detected in the pancreas from e13.5 to postnatal day (P) 30. A gradual increase in transcript levels was observed during development. Relative expression normalized to GAPDH is shown below the blot.

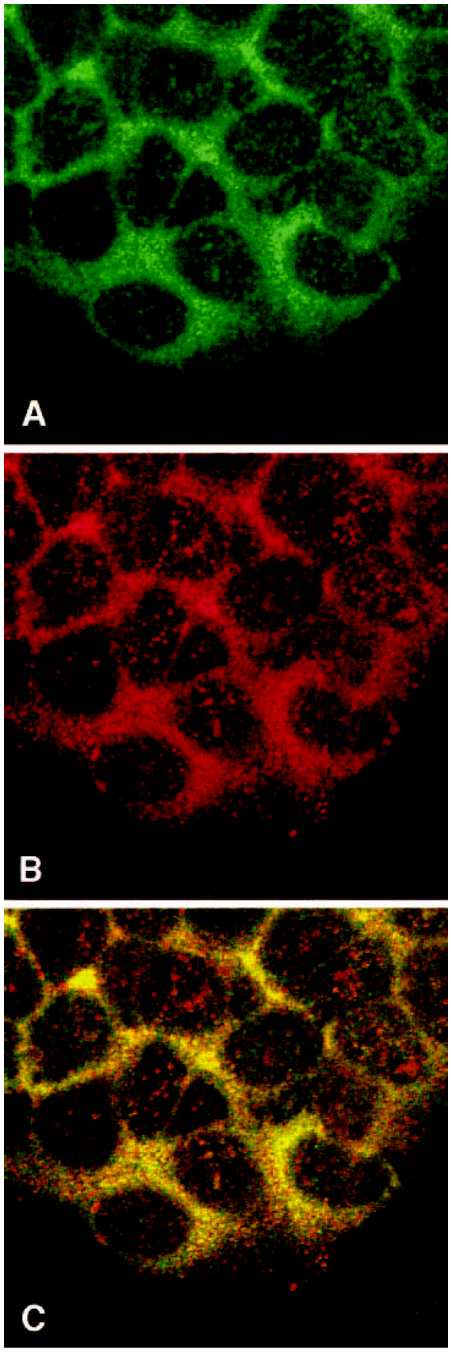

FIG 6.

Confocal microscopy localization of NNAT and insulin. NIT cells were stained with insulin (*A*) and NNAT (*B*). The merged image is shown in *C*. Most of the NNAT staining colocalized with insulin, whereas a minority of the NNAT staining did not, suggesting the presence of NNAT in another unidentified structure.

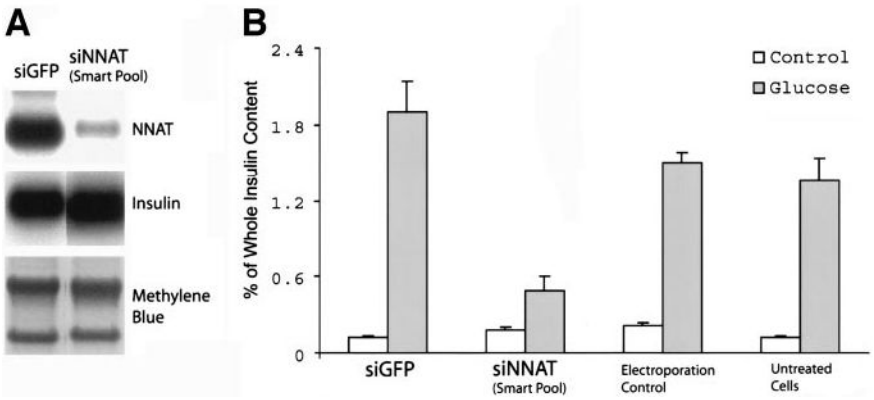

FIG 7.

Knockdown of *Nnat* in NIT cells and its effect on insulin secretion. *A*: Northern blot analysis of *Nnat* was used to confirm the potency of *Nnat* downregulation by the Smart Pool siNNAT. We observed >90% downregulation of the transcript, whereas the insulin transcript remained unchanged. Methylene blue staining was used as a loading control and also to assess the efficiency of the transfer. *B*: Insulin response to a glucose challenge. NIT cells were treated with either no (□) or 2.5 mmol/l (▨) glucose. NIT cells treated with Smart Pool siRNA showed impaired insulin secretion (only 2.7 × induction), even at a higher glucose concentration (25 mmol/l; data not shown). All control lanes responded to the glucose challenge, with the fold change varying from 15.5 (siGFP) to 7.0 (electroporation control) and 10.6 (untreated cells). Representative results are shown from three independent experiments. Data are means ± SE and represent the percentage of insulin secreted per whole insulin content.

TABLE 1

Primary and secondary antibodies used

Primary antibody	Source	Dilution	Secondary antibody	Source	Dilution	TSA	Tertiary complex	Dilution	Amplification molecule
Guinea pig anti-insulin	Linco Research	1:500–2,000	FITC or Cy3 donkey anti–guinea pig	Jackson	1:200 (FITC) 1:400 (Cy3)	No	NA	NA	NA
Rabbit anti-glucagon	Diasorin	1:500–2,000	Cy3 donkey anti-rabbit	Jackson	1:400	No	NA	NA	NA
Goat anti-neuronatin	Santa Cruz Biotechnology	1:100	Alexa 555 donkey anti-goat	Jackson	1:400	No	NA	NA	NA
Rabbit anti-BETA2	Courtesy of J. Drouin (IRCM, Montreal, Canada)	1:5,000	Biotinylated donkey anti-rabbit	Jackson	1:400	Yes	Streptavidin-HRP	1:200	Alexa488-Tyramide
Rabbit anti–β-galactosidase	Abcam	1:5,000	Biotinylated donkey anti-rabbit	Jackson	1:400	Yes	Streptavidin-HRP	1:200	Alexa488-Tyramide
Rabbit anti-PDX1	Courtesy of C. Wright (Vanderbilt U, Nashville, TN)	1:5,000	Biotinylated donkey anti-rabbit	Jackson	1:400	Yes	Streptavidin-HRP	1:200	Alexa488-Tyramide
Rabbit anti-NGN3	Courtesy of M. German (UCSF, San Francisco, CA)	1:5,000	Biotinylated donkey anti-rabbit	Jackson	1:400	Yes	Streptavidin-HRP	1:200	Alexa488-Tyramide
Rabbit anti- Pax6	Chemicon	1:5,000	Biotinylated donkey anti-rabbit	Jackson	1:400	Yes	Streptavidin-HRP	1:200	Alexa488-Tyramide
Rabbit anti-Nkx6.1	Courtesy of M. German (UCSF, San Francisco, CA)	1:5,000	Biotinylated donkey anti-rabbit	Jackson	1:400	Yes	Streptavidin-HRP	1:200	Alexa488-Tyramide
Mouse anti-Nkx2.2	DSHB	1:100	Biotinylated donkey anti-mouse	Jackson	1:400	Yes	Streptavidin-HRP	1:200	Alexa488-Tyramide
Goat anti- NNAT	Santa Cruz Biotechnology	1:50	Biotinylated donkey anti-goat	Jackson	1:400	Yes	Streptavidin-HRP	1:200	Alexa488-Tyramide
Mouse IgG	Santa Cruz Biotechnology	1:100–400	Biotinylated donkey anti-mouse	Jackson	1:400	Yes	Streptavidin-HRP	1:200	Alexa488-Tyramide
Rabbit IgG	Santa Cruz Biotechnology	1:100–400	Biotinylated donkey anti-rabbit	Jackson	1:400	Yes	Streptavidin-HRP	1:200	Alexa488-Tyramide
Goat IgG	Santa Cruz Biotechnology	1:100–400	Biotinylated donkey anti-goat	Jackson	1:400	Yes	Streptavidin-HRP	1:200	Alexa488-Tyramide

TSA, tyramide signal amplification; Jackson, Jackson ImmunoResearch; DSHB, Developmental Studies Hybridoma Bank. Alexa499-Tyramide was purchased from Molecular Probes.